International Journal of Innovative Research and Scientific Studies, 7(4) 2024, pages: 1693-1710

IJIRSS International Journal of Innovative Research & Scientific Studies

ISSN: 2617-6548

URL: www.ijirss.com

Fiber laser-based two-wavelength sensors for detecting temperature and strain on concrete structures

Nurzhigit Smailov[1*], Torekhan Zhadiger[2], Yerlan Tashtay[3], Askar Abdykadyrov[4], Aziskhan Amir[5]

[1,2,3,4,5]*Department of Electronics, Telecommunications and Space Technologies, Satbayev University, Almaty, Kazakhstan.*

Corresponding author: Nurzhigit Smailov (*Email: n.smailov@satbayev.university*)

Abstract

In this article, we discuss the scientific research we conducted to ensure information security on concrete structures using the fiber Bragg grating method. As a result, guided by the experiences of other researchers and their results in our studies, the main hazards were identified, and the influence of temperature and deformation sensors in concrete was studied. The work determines the dependence of temperature on the optical cable and its effect on concrete deformation. It also studies the change in the internal structure of the optical fiber when exposed to concrete, and in comparison, with non-concrete optical fiber. In the experimental chapter, conducted on laboratory bench, we consider and study the signal transmission structure of an optical sensor that experiences deformation upon impact with concrete and such fibers. Graphic data was obtained using the OptiSystem program. During the process of determining the optical power of the sensors, we discovered that the higher the vibration during signal transmission, the higher the power of the optical data acquisition system unit. The results presented in this paper show the promise of fiber optics in other environments, as well as new discoveries in the construction industry and the successful use of electrical laser sensors to maintain temperature and stress in a variety of concrete structures, including cooling towers in nuclear and thermal power plants.

Keywords: Concrete, Fiber Bragg Grating, Laser, Optical fiber, OptiSystem, Temperature, Touch sensor.

DOI: 10.53894/ijirss.v7i4.3481
Funding: This research is supported by Ministry of Science and Higher Education of the Republic of Kazakhstan (Grant number: AP19679041).
History: Received: 3 April 2024/**Revised:** 27 July 2024/**Accepted:** 19 August 2024/**Published:** 2 September 2024

Competing Interests: The authors declare that they have no competing interests.
Authors' Contributions: All authors contributed equally to the conception and design of the study. All authors have read and agreed to the published version of the manuscript.
Transparency: The authors confirm that the manuscript is an honest, accurate, and transparent account of the study; that no vital features of the study have been omitted; and that any discrepancies from the study as planned have been explained. This study followed all ethical practices during writing.
Institutional Review Board Statement: Not applicable.
Publisher: Innovative Research Publishing

1. Introduction

The field of structural health monitoring (SHM) has witnessed significant strides in recent years, driven by the pressing need for enhanced infrastructure resilience and safety. Concrete structures, as integral components of our built environment, demand meticulous attention to their structural integrity to mitigate potential risks and ensure longevity. In this context, the development and application of precise and reliable sensors for monitoring temperature and strain within concrete structures have become paramount.

Traditional methods of monitoring temperature and strain often face challenges such as limited spatial resolution, susceptibility to environmental conditions, and the need for frequent maintenance. To overcome these limitations, optical fiber sensors have emerged as promising candidates, offering advantages such as high sensitivity, immunity to electromagnetic interference, and the ability to cover large areas with a single sensor network. Among the different optical sensing methods, using two-wavelength fiber laser sensors is a new and effective way to check both temperature and strain in concrete structures at the same time.

In this work, a method using optical Bragg gratings with a combination of several fiber lasers to form the required resonator structure is proposed. This technology simultaneously acts as a laser resonator and a microfluidic channel, which reduces the maximum temperature and power to optimal values. The OptiSystem software environment simulated the temperature variation of the concrete medium. The primary goal of this study is to calculate the deformation and temperature using fiber-optic sensors and to conduct a comparative analysis based on experimental data. Also, dual-polarized sensors, which can be used in many fields such as smart design and smart robotics, can be used to measure deformation and temperature at the same time [1]. It is known that the rapid development of economical and reliable sources that emit coherent radiation in the mid-infrared wavelength zone is the main driving factor for the development of miniature gas sensors. Configurations require periodic calibration to maintain repeatability. We can solve this problem by introducing detection methods that encodes the gas concentration by frequency [2, 3]. It is possible to use anti-corrosion, high-explosion-proof sensors that provide the possibility of convenient transmission of information to the enterprise, which gives recognition to the fiber-optic technology industry. At this time, measuring parameters using two-wave fiber laser sensor research lines was considered for determining temperature and deformation. In addition, there are also methods for creating a parallel integrated ultra-short FBG type II (PI-US-FBG) using laser point technology [4].

2.Background

In the paper Theodosiou, et al. [5] fiber optic sensing technology is shown to address the limitations of traditional electronic monitoring in concrete structures through enhanced scalability, distributed sensing capability, and immunity to electromagnetic interference, providing accurate measurements in critical areas of a building, but this work lacks data on the effects of concrete optical fiber parameters in concrete structures. Focusing on humidity monitoring in concrete structures, paper [6] details the design and testing of a novel packaging for an experimental fiber optic sensor. Functional evaluations confirmed the minimal impact of the encapsulation on sensing performance, validating the design choices and initial assumptions; however, this method is less efficient because it does not consider the effect of temperature on the optical fiber when measuring in concrete structures.

Addressing the critical need for accurate rebar corrosion detection in wet environments, paper [7] investigates the tilted fiber Bragg grating (TFBG) as a novel sensor. The authors show that the TFBG's can effectively track early-stage deterioration through in-situ monitoring and accelerated corrosion using an impressed current technique. Notably, a 28.9% rebar mass loss within 24 hours resulted in a distinct and consistent red shift in the cladding resonant wavelengths. Intriguingly, higher-order resonances exhibited a significantly larger shift compared to their lower-order counterparts, highlighting enhanced sensitivity to incipient corrosion. These results show that TFBGs have a lot of potential as corrosion sensor for steel rebars that are both very sensitive and very strong. This could lead to better ways to check on the health of structures and do preventative maintenance in wet infrastructure. Given the widespread concern regarding concrete structure deterioration, the inherent advantages of fiber optic sensors offer promising potential for enhanced crack damage detection accuracy and precision. This paper [8] presents a critical review and comparative analysis of diverse fibre optic crack detection approaches. This work further evaluates the compatibility and sustainability of cutting-edge fiber optic sensors for concrete damage sensing, contributing to the development of robust and effective monitoring strategies. It is worth noting that a shortcoming of the works [7, 8] is the imprecision of the methods without considering the parameters and dependencies of optical fiber in specific circumstances and arrangements in the context of concrete structures.

This study investigates the signal transmission behavior of optical sensors under thermal and mechanical stress induced by concrete impact. Elevated temperature cause the signal weakening and deformation, with the degree of deterioration surpassing acceptable limits at higher temperatures. The analysis focuses on the signal transmission structure of the sensor and its response to deformations arising from the impact. Additionally, the investigation highlights the correlation between vibration intensity during signal transmission and the required power unit for optical data acquisition systems, indicating a direct relationship between increased vibration and higher power demands.

The findings presented in this research hold significant potential for the development of advanced monitoring systems for cooling towers in both thermal power plants (TPP) and nuclear power plants (NPP). Employing the acquired data, such systems could facilitate enhanced maintenance practices and enable the timely detection of structural defects and material degradation within the cooling towers. The resulting system architecture and the underlying data analysis methodologies would serve as valuable resources for further scientific research, particularly in the domains of metal coatings and concrete structures, benefiting both established researchers and students in these fields.

3.Materials and Methods

Laser communication is considered the best way to connect high-bandwidth data-efficient devices, although it has some drawbacks. This forming process utilizes reliable, secure, and full-duplex additive technology. This technology has advantages, but a note is made about the disadvantages of installation and assembly.

By depicting the effect of changes in temperature and mechanical force, microbending affects and deforms the resulting optical fiber, sheath, and core, which leads to a change in the refractive index of the optical fiber:

$$\frac{\Delta n}{n} = \frac{1}{n}\left(\frac{\partial n}{\partial T}\right) p\Delta T + \frac{\delta n}{n}\delta n(1)$$

Where n is the refractive index of the core of the fiber;Δn - change in the refractive index;($\frac{\partial n}{\partial T}$)pis a partial derivative concerning temperature that describes the correction; ΔT is the density of quartz glass; δn is the refractive index due to photoelasticity.

Here is the photoelasticity effect due to single-mode optical cable according to the refractive index G.652 standard:

$$\frac{1}{n}\left(\frac{\partial n}{\partial T}\right) p = 0{,}68 * 10^{-5} {}^{\circ}C^{-1}(2)$$

In the process of transmitting information in the form of light through a sensor and a communication network, the basis of the signal's ability to break is accommodated in the information sensor. The sensor operate on the principle that the characteristics of the laser radiation spectrum, along with its ability to connect the sensor to adjustment factors, temperature, pressure, vibration, and external factors in the detection device can change the characteristics of the optical flow. Currently, due to the use of fiber-optic communication, it is possible to use 1310 and 1550 nm lasers in these information sensors.

We can also measure the output power of the fiber laser using copper-coated optical fiber. The metal layer partially scatters and absorbs the optical beam passing through the fiber core of the sensor to achieve this. Then the change in electrical resistance proportional to the induced heat is measured. You can also adjust the sensitivity by changing the radius of curvature of the fiber. We can also use digital fiber heating model to calculate the specific and flexible optical loss coefficients [9].

A new structure is called a feedback and integrated fiber network to receive information. This structure aims to replicate the physical properties of the medium. Even the first reflectors did not use feedback and long fiber coils. Currently, all the recording characteristics for emission around 1550 nm have been added to the application in this new structure. We have started rearranging new reflectors near the consumption touch of the EDFA lasers. The larger the deviation distance and the shorter the period, the greater the loss in all fibers across the area. However, in multi-mode fibers, there is a possibility of losses to meet the conditions of interaction with each other. Even here, in small-diameter regions, the distribution of regularity is characterized by lossy or emitted wave. The effect of the EDFA amplifier after power regeneration was analyzed in the Matlab program.

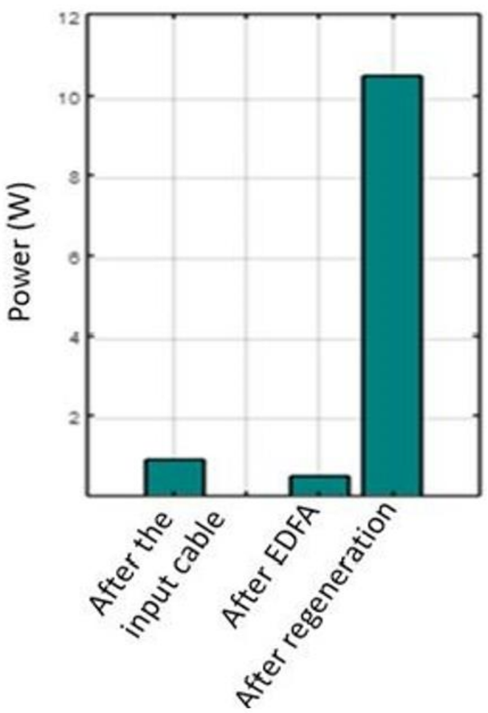

Figure 1.
Cable length 100 km, EDFA gain 20 dB.

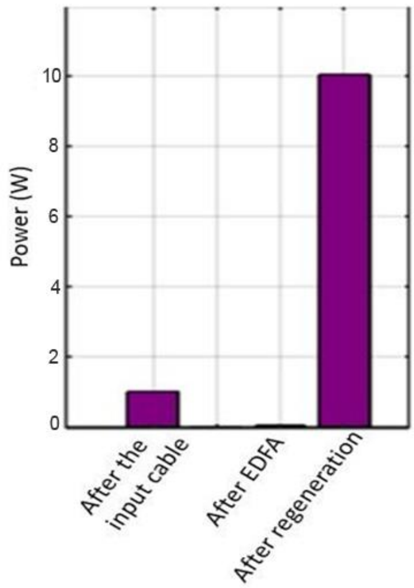

Figure 2.
Cable length 50 km, EDFA gain 15 dB.

Figures 1 and 2 compare execution programs at different speeds for fiber applications. The second calculation analyzes the physical phenomenon of the fibers and incorporates them into the light transmission characteristics window. It shows multiple light patterns propagating through the fibers and determines the size of these patterns for calculation and the rotation of the windows with each other, thereby determining their relationship. Deformation images sometimes require fibers to be comfortably addressed in a windowed curvature, leading to the importance of initial fiber placement and large shear rates. The transmission medium of this information will have sufficient protection against micro-benders from fiber protection materials.

3.1. Conditions of Optical Cable Deformation with Temperature

Currently, there are various methods for testing the dynamic properties of materials to determine the parameters of deformation and fracture models, such as the Hopkinson, Kolsky, and Taylor methods used for impact bending and others. It is important to note that these methods have their limitations due to high strain rates and uncertainty in the relationship between shear strength and direct tensile strength, especially for plastics. In certain areas, fibers can emit new light modified by acrylate [10]. The degree of deformation is determined by the amount of light that bends across the region as it enters the sensor through the mode filter area. As the bending radius of the fiber and movement in the bending plate change, the proportion of light transmitted through the cladding also changes. After leaving the deformed region, the light travels through the coating to the filtering region, where the region-propagating light disappears. Movement modulates the amplitude of the light reaching the receiver. There is also a new method for creating sapphire fiber Bragg nets (SFBGs) using the femtosecond laser direct recording technique, i.e., linear scanning (LbL) and point scanning (PbP) methods. And after the high-temperature test, the inert gas hermetic packaging method can be used to remove the loss spots that appear on the surface of the sapphire fiber. This has significantly improved the long-term thermal stability of SFBG. As a result, such SFBGS can be used in many industries, including metallurgy, energy, and aviation [11]. We also recommend an effective monolithic fiber laser in some cases, which embeds fiber Bragg mesh mirrors (FBGs) directly into the active fiber using a femtosecond laser [12].

Many fiber-optic technologies have been developed to measure temperature, and some sensors are commercially available. In the past, laboratory sources of infrared (IR) radiation were the first medium-temperature light sources or electric light beams. Currently, solid-state and molecular gas lasers based on controlled or fixed-frequency infrared radiation have also been reported. To record the radiation of the near-infrared region (up to 1.3 μm), photo plates are used. And depending on the distance of the received light from the immediately received area, it is modulated with reference to the light approaching the far area. The fiber-optic measuring device has a smart capability to find thermodynamically specific hot spots, evaluate their changes, and measure the Kelvin temperature. Compared to other sensors, the fiber-optic measuring device is explosion-proof, resistant to electrical interference, and has an unlimited operating temperature range. Counters are made of non-conductive materials, which can be used at low and high voltages. Spectral fiber optic sensors can be used to detect voltage, pressure, temperature, chemical composition, haze, color, and other measured values. There are two different methods of operation for the sensors: a sensor with a single sensing point at the end of the fiber and a distributed detection method. A sensor with a single sensing point at the end of the fiber is the simplest form of fiber optics, consisting of an indicator at one end of the fiber, a light source, and a sensor at the other end [13].

Researchers have conducted several studies to measure temperature. Optical sensors are used to measure the temperature in this area. Rayleigh scattering, combined scattering, optical fiber Brillouin scattering, and Raman scattering, and optical sensors for evaluating temperature changes are placed. These sensors are used for temperature glasses in temperature measuring systems and other stages, and help to provide quality measurements [14, 15].

The Matlab program determines the temperature dependence of optical power and distance:

$$\mathrm{P(z)} = \mathrm{P(0)} * \exp(-\alpha * z) \qquad (3)$$

The formula is the standard mathematical description of light attenuation in an optical fiber. It is based on the Bouguer-Lambert-Beer law, which describes the attenuation of light as it passes through matter. The law is named after Pierre Bouguer, Johann Lambert, and August Beer, who contributed greatly to the development of photometry and optics.

In the context of optical fibers, α is commonly referred to as the attenuation or loss factor and is measured in decibels per kilometer (dB/km). The value of α can depend on many factors, including light frequency, temperature, and material properties of the fiber. Figure 3 shows the absorption and temperature dependence of power and distance in the optical slice.

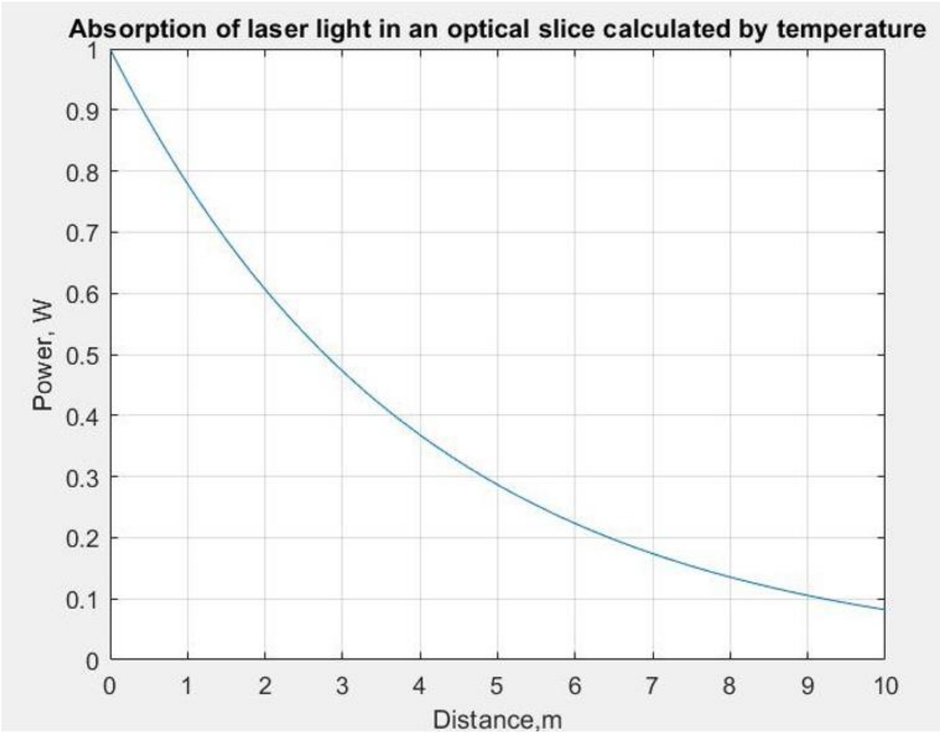

Figure 3.
Absorption and temperature dependence of power and distance.

Innovative developments in structural design, insulation, and fiber optic sensor implementation technologies are driving the phenomenon. Most of the new additions in the field of geotechnical monitoring have been fiber-optic communication [16].

Karaganda coal mines belong to the super category of gas and dust explosions, where accidents often occur, resulting in the deaths of workers. There is a need to develop a monitoring system, to determine the geotechnical situation with the ability to monitor the necessary parameters in real-time. Unfortunately, there are no original developments in the Republic of Kazakhstan, the developments are limited only to theoretical research and preliminary work on the creation of laboratory models. Mainly a highly sensitive material thermal expansion sensor, the optical structure is composed of an interferometric fiber sensor and an erbium alloy ring fiber laser as the light source. The sensor is made up of a combination of single-model mirror fibers with a hollow core and without a core. Two different sizes on different bases in metals represent performance in terms of the material's sensitivity to expansion [17, 18].

We used the following components from the OptiSystem to simulate the temperature effect on the optical signal: CW Laser, Dual Port WDM Analyzer (DPWDMA), Er-doped fiber laser (EDFL), Optical Spectrum analyzer, and Optical power meter. CW Laser is used as an optical signal source with a definite wavelength value. DPWDMA estimates the signal and the noise power for each optical signal channel based on the resolution bandwidth for each input port. We used EDFL as a source for coherent light signal generation. The temperature interdependence, or the cross-sections σa, and radiation in EDFL are expressed by a change in the absorption coefficients. The optical spectrum analyzer and optical power meter output spectral analysis and the value of the optical signal power under the temperature effect.

The practical setup for determining the deformation of concrete consists of an optical signal source, a single-mode cable embedded in a concrete object, and an optical signal receiver.

4. Results and Discussion

4.1. Bending Strain Sensor Based on Bragg Gratings

Optical Bragg gratings are proposed, with a combination of multiple fiber lasers forming the required resonator structure.

A feature of this structure is its ability to reflect light only in a narrow spectral range. Basically, the Bragg structure in an optical fiber is a one-dimensional photonic crystal. Thus, we calculate the Bragg-Wolf law and the resonant (Bragg) wavelength of the reflected light:

$$\lambda_B = 2n\Lambda \qquad (4)$$

Where Λ is the period of the lattice, n is the average (effective) refractive index for the mode propagating along the fiber, λ_B is the central wavelength of the reflected light stream, called the Bragg wavelength [19].

Also of practical importance is the width of the grid. In classical theory, the total width of the grid is determined by the spectral distance between the first zeros of the reflection coefficient:

$$\Delta\lambda = \frac{2\lambda_B}{N_B}\sqrt{1} + \left(\frac{k_B}{\pi}\right)^2 \qquad (5)$$

Where $N_B = \frac{L}{\Lambda_B}$ is the number of lattice lines, k_B is the coupling constant, or lattice strength, $\Delta\lambda$ is the width of the general half range.

Using Bragg sensors, its shape can be reconstructed with great accuracy, and the places of critical deformations can be determined. We can estimate the total deformation of two orthogonal sensors during the fiber optic cable's bending using the following formula:

$$\varepsilon = \varepsilon_1 - \varepsilon_2 = \frac{d}{R} \qquad (6)$$

Where ε_1 and ε_2 are the amount of deformation of the upper and lower meshes, respectively, dis the distance between the cores, R is the bending radius of the fiber. In terms of the Bragg wavelength λ_B taking into account the Photoelasticity coefficient of the fiber light conductor, the total wavelength change Bragg gratings $\Delta\lambda$ can be written:

$$\Delta\lambda = \frac{\lambda_B(1-p_e)d}{2R} \qquad (7)$$

The change in wavelength is usually monitored using a variable wavelength source, a spectrally insensitive photodetector, or a broad spectrum source and a spectrometer that measures the spectral density of the reflected radiation, since FBG parameters change slowly. To keep an eye on fast changes in FBG parameters that happen in microseconds and fractions of microseconds, simple probes can't give a good picture of how the resonant wavelength changes over time. Instead, the power of the FBGs reflected radiation must be used. Double-clad rare-earth-doped fiber lasers have become the focus of much research due to their high-quality single-mode beam and ease of use. This opens the way for a method in which the fiber microstructure serves as both a laser microcavity and a Micam microfluidic channel.

Because the polymers film's refractive index is higher than that of silicon dioxide, it is able to support the "Whispering Gallery" mode. In addition, a single-frequency, low-ring cavity fiber laser operating in the C and L bands is of great importance [20-23].In current diagnostic methods outlined in scientific studies, an optical source is employed, either a wavelength-tunable laser or a broadband source. However, utilizing a laser with tunable wavelength might not provide adequate speed for measuring the central wavelength in processes with high pulse rates. On the other hand, the reflected signal power from the FBG may decrease when using the broadband radiation source [24].

4.2. Thermal Resistance of Bragg Gratings

One of the necessary parameters of Bragg gratings operating in the extended temperature spectrum is their thermal stability, which is the ability to maintain their original characteristics during and after exposure to high temperatures. In the vast majority of cases, the operating mode of optical fibers does not exceed 85°C, which allows the use of ordinary optical fibers with an acrylate protective coating for these purposes. The same requirement applies to Bragg gratings that do not work at high temperatures. But even with such operational agreements, additional stabilization of grid parameters is required for several tasks, such as high-precision sensors. Use optical fiber with a special heat-resistant coating, such as polyimide varnish or metal, for tasks where the temperature order exceeds the specified values [25]. Creating regenerated Bragg gratings is a widely discussed way to ensure high thermal stability. Bragg gratings written with molecular hydrogen in their cores are thermally annealed at very high temperatures, resulting in a grating that remains stable at 1000°C. However, the reflection level of such gratings is naturally low, and the development of their creation is very difficult, so they did not find real practical use, only laboratory exhibits remained. In other equal arrangements, the value of their changes appears to be a refraction due to the thermal stability of the induced index. Therefore, it is necessary to cover the thermal stability of the Bragg grating in order to operate even at low temperatures for a long-term flow. Various fields of industrial production and military defense widely use powerful fiber lasers. In recent decades, when developing fiber lasers, the thermal effect has always been one of the biggest obstacles. To increase productivity, it is critical to study the characteristics of temperature and overcome heat restrictions. In this regard, the slit beam formation method is also used for femtosecond laser point (PbP) recording of highly localized fiber Bragg lattices (FBGs). Well, a circuit that combines a capillary tube with an elastic cavity can be used to create a thin fiber laser hydrophone (FLH) with static pressure equalization, high sensitivity to dynamic pressure, and wideband flat response [26-28]. The examination of physical phenomena reveals a relationship between fiber optical and micromechanical structures and visible phenomenon and effects in semiconductor structures, including deformations, thermal phenomena, optical effects, and mass transfer effects of charge carriers. At the same time, a large number of coherent phenomena are observed in nanostructures, although they often lack temporal and parametric stability [29].

Some works also feature fiber laser temperature sensors based on temperature dependence in the Whispering Gallery Mode, based on a micro-resonator. Meanwhile, TM3 + alloy passive mode synchronization fiber laser based on a nonlinear polarization rotation mechanism and Cascade long-term fiber mesh (LPFG) has been used to generate an ultra-fast output signal in cylindrical vector mode (CV). The research concentrates on the issue of stimulated Brillouin scattering (SBS), which arises from the use of two beams in a single-mode optical fiber at wavelengths of 1310 and 1550 nm. Due to limitations on the intensity and energy of signals caused by SBS in main fiber optic lines, a search is underway for ways to reduce this impact [30-33]. The research shows that pre-saturating normal telecommunications optical fibers with hydrogen significantly increases their photosensitivity, allowing the effective use of fiber-optic Bragg gratings in various fields, including telecommunications and seismology. Experimental results confirm the increased photosensitivity of such fibers, which expands the potential for their use as highly sensitive sensors in extreme conditions [34]. Effective simulation of the first principle with the self-compatibility of interferometric fiber laser feedback sensor: it is known that the interferometric fiber laser feedback sensor consists of distributed Bragg reflectors/distributed feedback, where (DBR/DFB) is a fiber laser and an external sensitive feedback element. The broadband vibration sensor uses a reflected over-inclined fiber mesh (ExTFG) with a compressed beam. The two ends of the reflected ExTFG are fixed, and a piece of fiber mesh is suspended, thus forming a compressed beam structure. The resonant frequency and vibration mode of the sensor presented there can be calculated using digital calculation and software modeling [35-38]. It has been proven that diode autoinjection and distributed feedback (DFB) lasers can be used for highly sensitive acoustic emission (ae) detection using the fiber interferometric Fabri-pen sensor (FPI). Additionally, the use of various methods for measuring high-speed load parameters, such as a tensometric sensor, a fiber Bragg mesh located on a metal measuring rod, and an interferometer that monitors the movement of the free border of the end of the rod also gives great results [39, 40]. Although, using optical signals and Bragg gratings has a high efficiency and accuracy in determining deformation and temperature in concrete structures, this method is economically expensive and technically difficult to implement. This study reveals opportunities for technological advancement and its effective use in a variety of the fields [41]. The study demonstrates that the use of fiber optic sensors, including hydrogen-pre-saturated Bragg gratings, in construction and overhead power lines can accurately monitor strain and stress, providing high sensitivity and robustness to extreme conditions [42, 43].

The use of workpieces with different values of the upper temperature makes it possible to create a sensor with the desired operating temperature. Table 1provides an example. A number of polycrystalline substances are listed, whose heat temperature permits their use in sensors for thermal protection of current-conducting parts with heat resistance classes of electrical insulating materials Y, A, E, B, F, H, 200, 220, 250 [31].

Table 1.
The heat resistance classes of electrical insulating materials and the types of working substances corresponding to them by melting point.

№	Electrical insulation heat resistance class materials	Temperature, which describes the heat resistance of materials of this class, °C,	Work object	Melting point of the working substance, °C
1	Y	90	1,4 dibromo benzene	87,5
2	A	105	Hydrocinnamic acid	101,5
3	E	120	Succinic anhydride	119,6
4	B	130	Urea	129-134
5	F	155	para-Nitroaniline	149
6	H	180	α – Camphor	178,4
7	200	200	Lactose	200
8	220	220	Anthracene	216
9	250	250	Glycine	247,2

4.3. Results and Modeling

The OptiSystem program is a growing package of simulation of optical communication systems that allows for the calculation of topics of development, testing, and virtual optimization of all variants of optical networks at the physical level of a wide range of optical networks, from television systems to backbone systems.

4.4. Experimental Setup

We used the following components from the OptiSystem program to stimulate the temperature effect on the optical signal: CW Laser, Dual Port WDM Analyzer (DPWDMA), Er-doped fiber laser (EDFL), Optical Spectrum analyzer, and Optical power meter. CW Laser is used as an optical signal source with a definite wavelength value. DPWDMA estimates the signal and the noise power for each optical signal channel based on the resolution bandwidth for each input port. We use EDFL as a source for generating coherent light signals. The temperature interdependence, or the cross-sections σa and radiation in EDFL are expressed by a change in the absorption coefficients. Optical spectrum analyzer and optical power meter output spectral analysis and the value of the optical signal power under the temperature effect.

The practical setup for determining the deformation of concrete consists of an optical signal source, a single-mode cable embedded in a concrete object, and an optical signal receiver. Figure 4 shows the temperature dependence model of the optical signal power used.

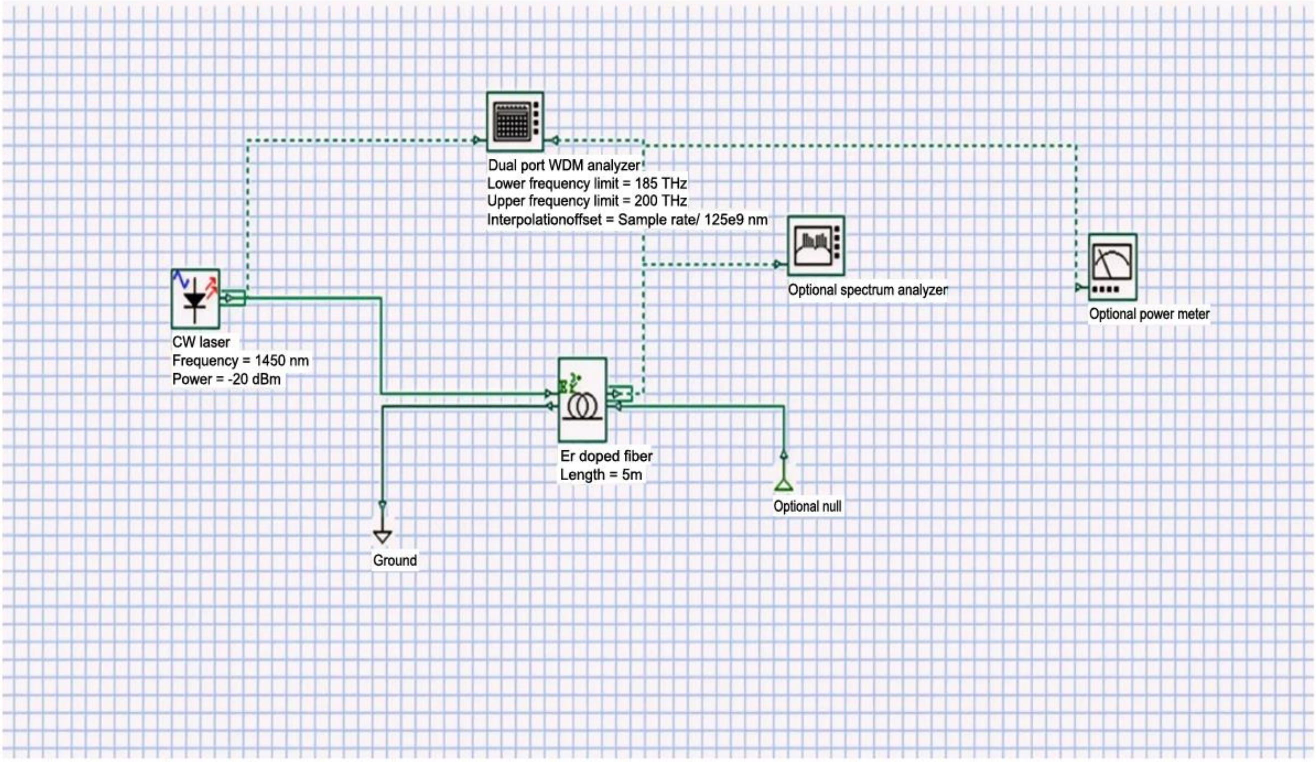

Figure 4.
General diagram of temperature dependence of optical signal power.

The interdependence of temperature in EDFA and (or σa and radiation cross-sections) is reflected by changes in absorption coefficients. Here, the results of temperature dependence are shown in Figure 5. Simulations are carried out using temperature, and the method of describing the absorption coefficient of EDFA in each result is used.

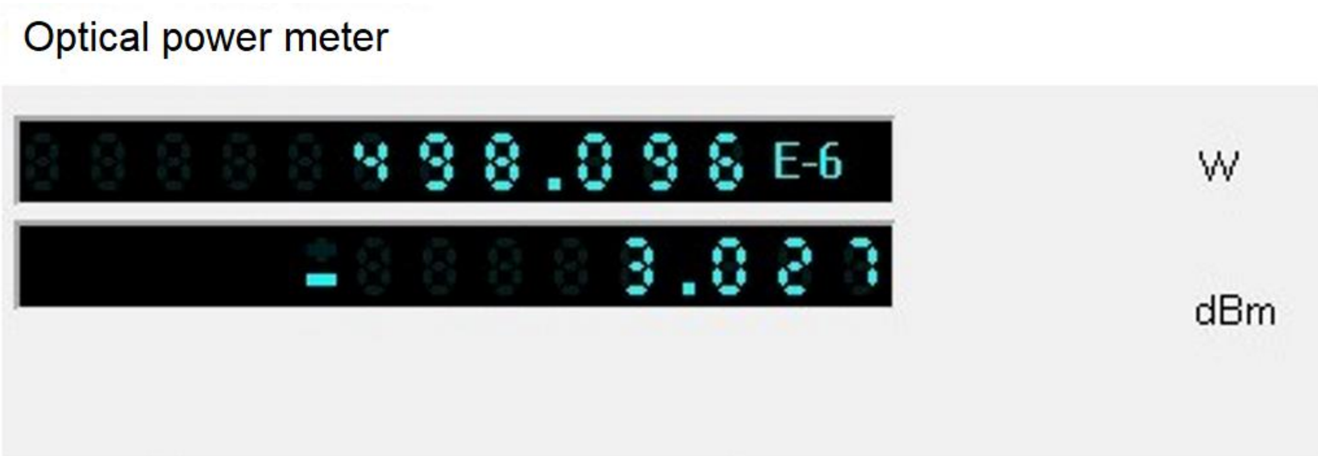

Figure 5.
Total optical power measurement.

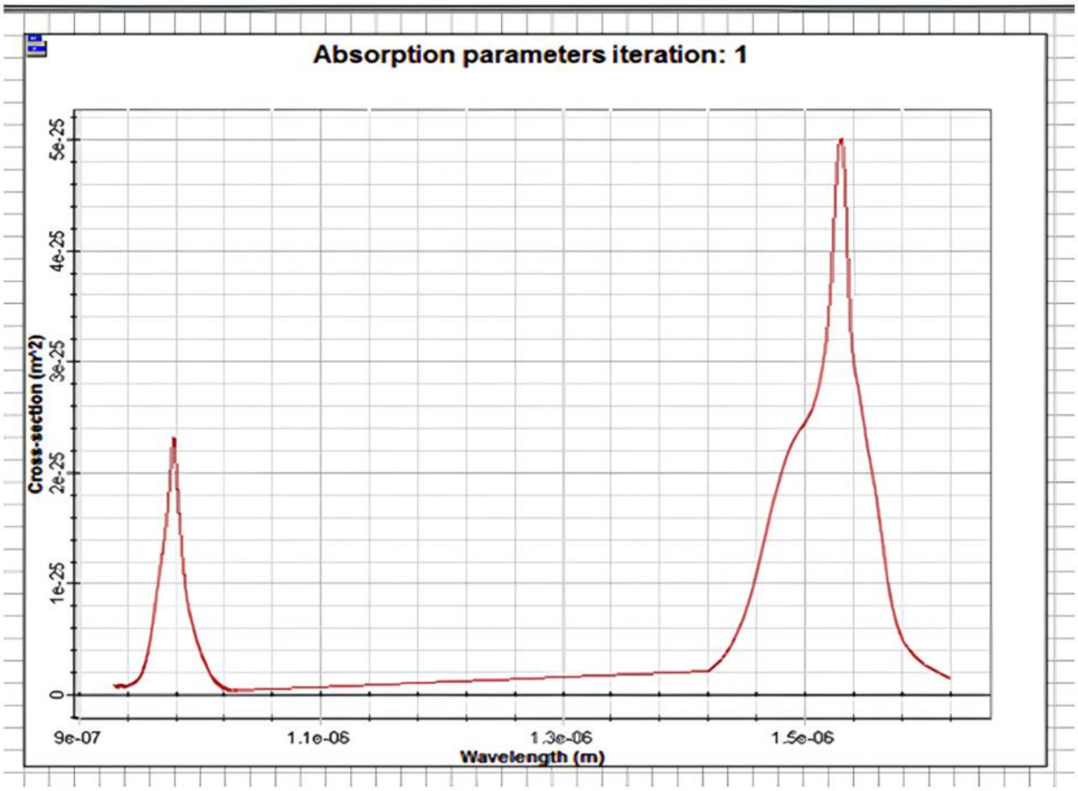

Figure 6.
Cross-section and wavelength absorption params recapitulation.

In Figure 6, the absorption wavelength indicates the wavelength of electromagnetic radiation that a substance is capable of absorbing. This feature is critical when analyzing spectra and studying the optical properties of materials. Together, these parameters provide an understanding of the interaction of light with matter at the molecular level, which is of enormous importance.

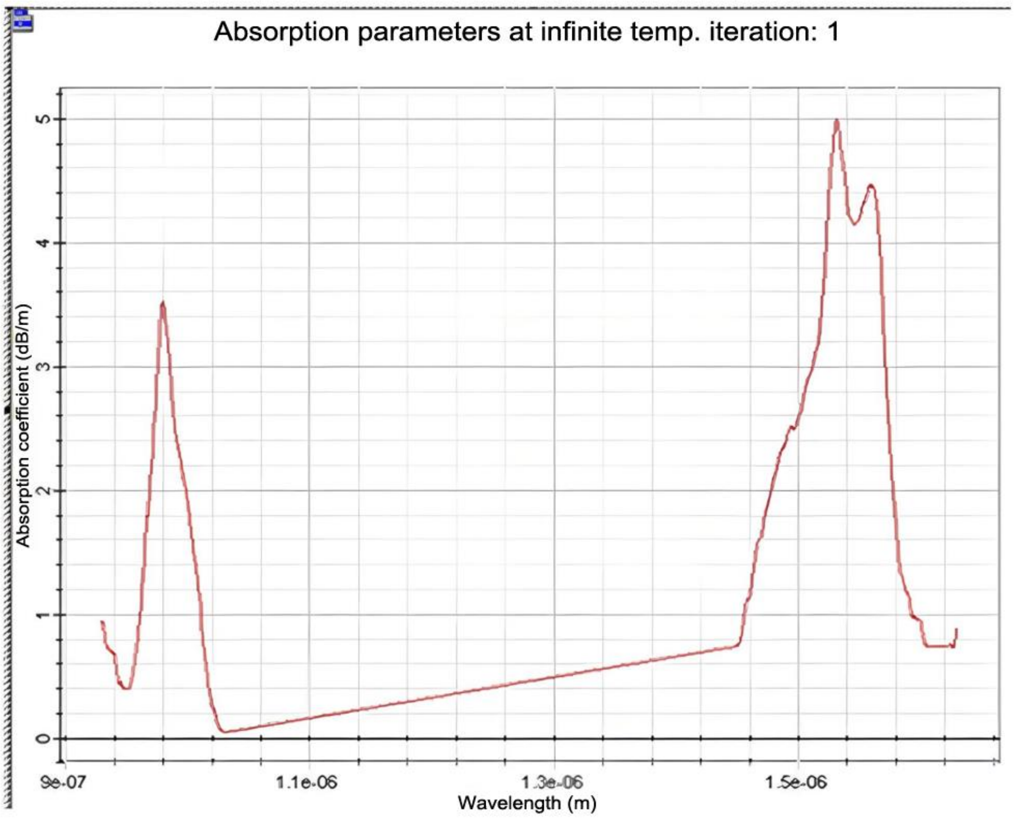

Figure 7.
Absorption coefficient graph at constant temperature.

Figure 7 displays a graph of the absorption coefficient at a constant temperature, which is a visual representation of the dependence of the absorption coefficient of a material on the wavelength of electromagnetic radiation at a fixed temperature. This graph allows you to analyze how the material interacts with different frequencies of light at the molecular level. The graph shows peaks and dips of the absorption coefficient depending on the wavelength, which indicates the specific properties of the substance.

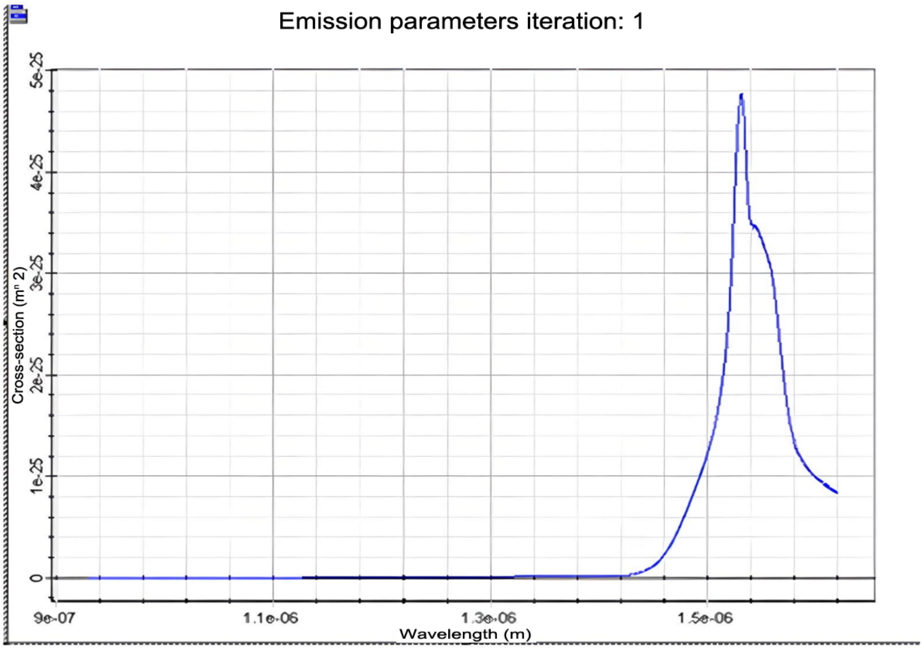

Figure 8.
Radiation parameters of cross-section and wavelength.

Figure 8 shows the radiation parameters, such as cross-section and wavelength, which are the key characteristics of electromagnetic radiation. The cross-section represents the probability of a particle interacting with radiation, and the wavelength determines the distance between points on the wave.

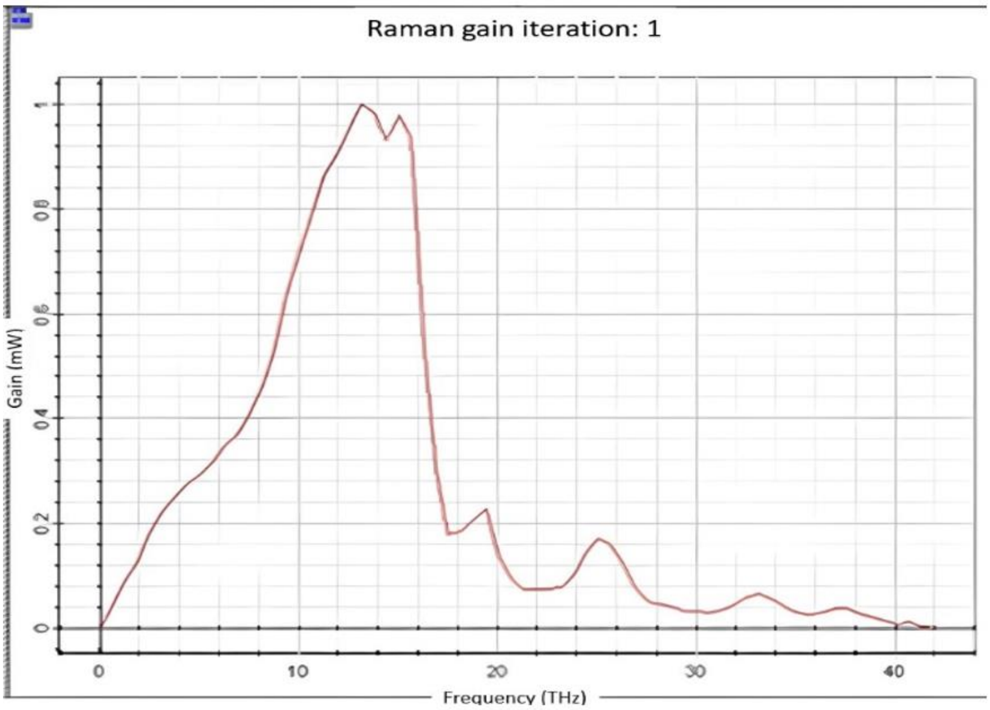

Figure 9.
The graph of frequency and gain in Raman scattering.

Figure 9 shows a graph of the frequency and gain in Raman scattering, which is a visual representation of the dependence of the radiation frequency on the gain in the process of Raman scattering. Raman scattering occurs when light interacts with matter, and when photons interact with molecules, causing a change in their energy and, consequently, a change in the frequency of the emitted light.

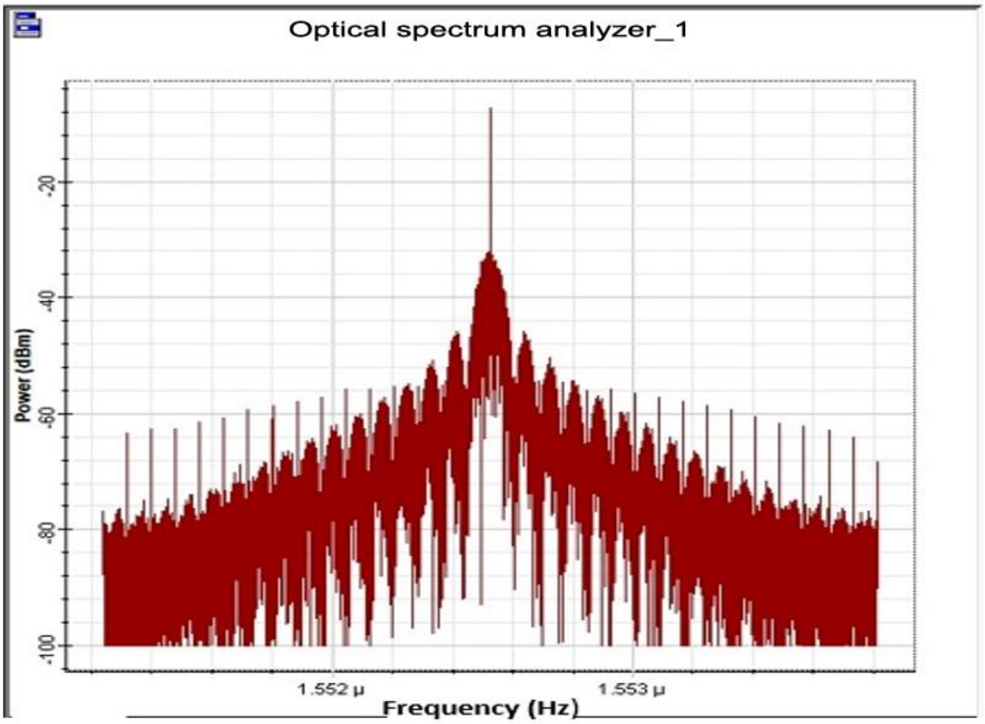

Figure 10.
Signal optical spectrum analyzer.

Figure 10 depicts the measurement and analysis of the optical spectrum of the light signal. Figure 10 displays the impact of light on different components based on their respective frequencies or wavelength.

4.5. Effect Of Fiber Optic Communication Cable with Concrete as a Result of Experimental Studies

In this section, we are developing the crucial role of optical fiber work in communication, and we are seeing an increase in the use of the optical communication technologies in oil field and mining operations. With the human flow mentioned below, optical fiber replenishment and maintenance in the field of communication resemble human-day notices.

Future technologies for non-destructive testing of concrete pavements using optical fibers will allow for development. With the use of optical technologies, it is possible to determine the mechanical coating of concrete, monitor the reception of stable concrete in the places of stabilization, and obtain information about changes in strong concrete. For experimental use, we chose a single-mode cable, which is shown before pouring concrete and the structure of the cable when it is located inside the concrete in Figure 11.

Figure 11.
Cable: a) single-mode cable; b) single-mode deformed cable.

We chose a single-mode cable that is used in Subscriber TV, Local Area Network (LAN), Fiber To The Home (FTTH) Table 2 presents the characteristics of the single-mode cable that we used to conduct the experiment.

Table 2.
General description.

Description:	Scope
The outer diameter is 3 mm Less reflection Good exchangeability High-temperature stability	Subscriber TV, LAN, FTTH

We are conducting an investigation into the technical characteristics of passive fiber optic devices. At this stand, we can measure the power of optical fibers and there is also an insulator, a splitter, an optical circulator, and a CWDM (Coarse Wavelength Division Multiplexing) multiplexer, optical radiation of a certain power is supplied at the input. We can reasonably infer that the deformation of the optical cable from the input power will alter the optical power at the output ports.

First of all, before experimenting, we observe the technical safety rules. We begin our research by ensuring the unconnected cells remain closed. First, we measure the optical power of an undisturbed single-mode cable Figure 12.

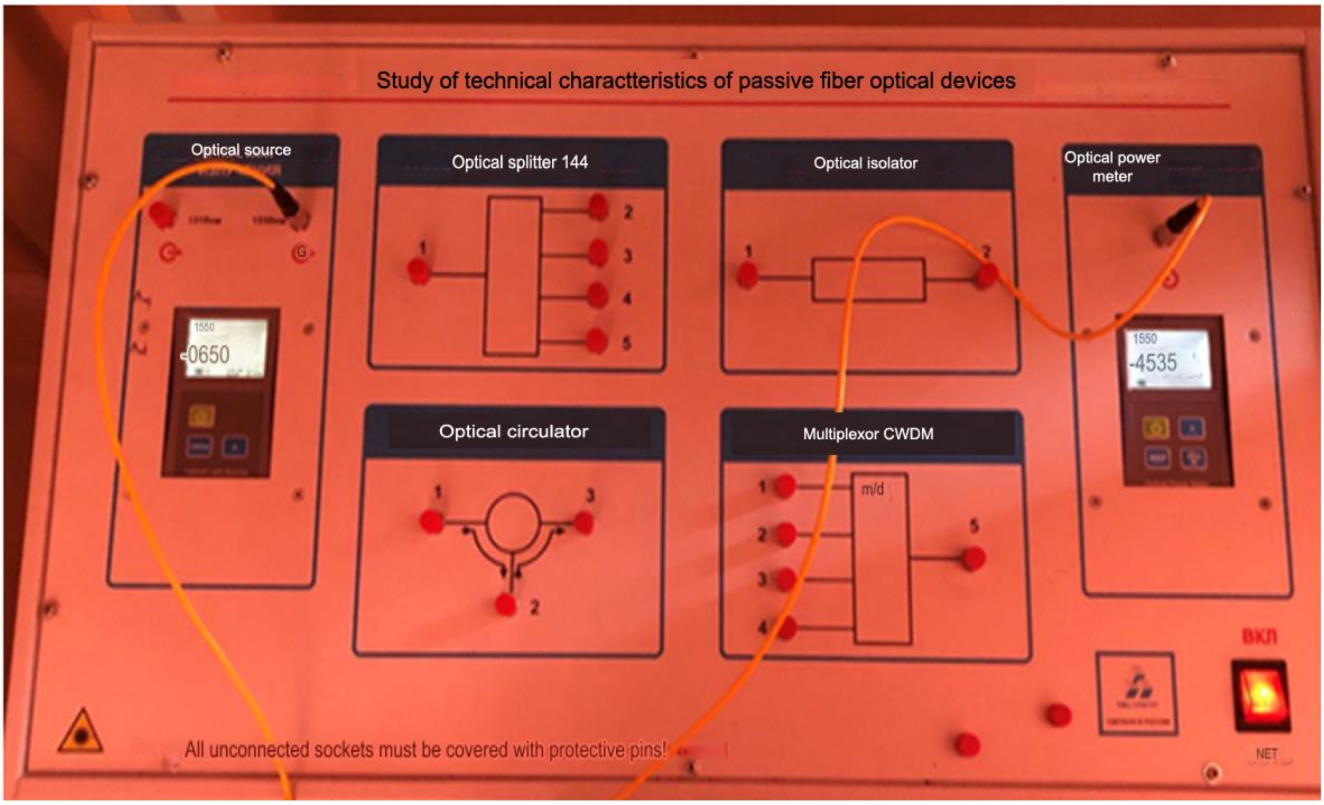

Figure 12.
Calculation of optical power without optical deformation.

Tables 3-4 present the wavelengths of 1310 nm and 1550 nm, sampling frequency and input signal level, and the output level at which it does not integrate with the concrete and does not deform.

Table 3.
Results at 1310 nm wavelength.

Input 1310nm	Output 1310nm
0.27kHz – 6.50dBm	47.35 dBm
100kHz – 6.50dBm	47.45 dBm
200kHz – 6.50dBm	47.53 dBm

Table 4.
Results at 1550nm wavelength.

Input 1550nm	Output 1550nm
0.27kHz – 6.50dBm	45.35dBm
100kHz – 6.50dBm	45.45 dBm
200kHz – 6.50dBm	45.56dBm

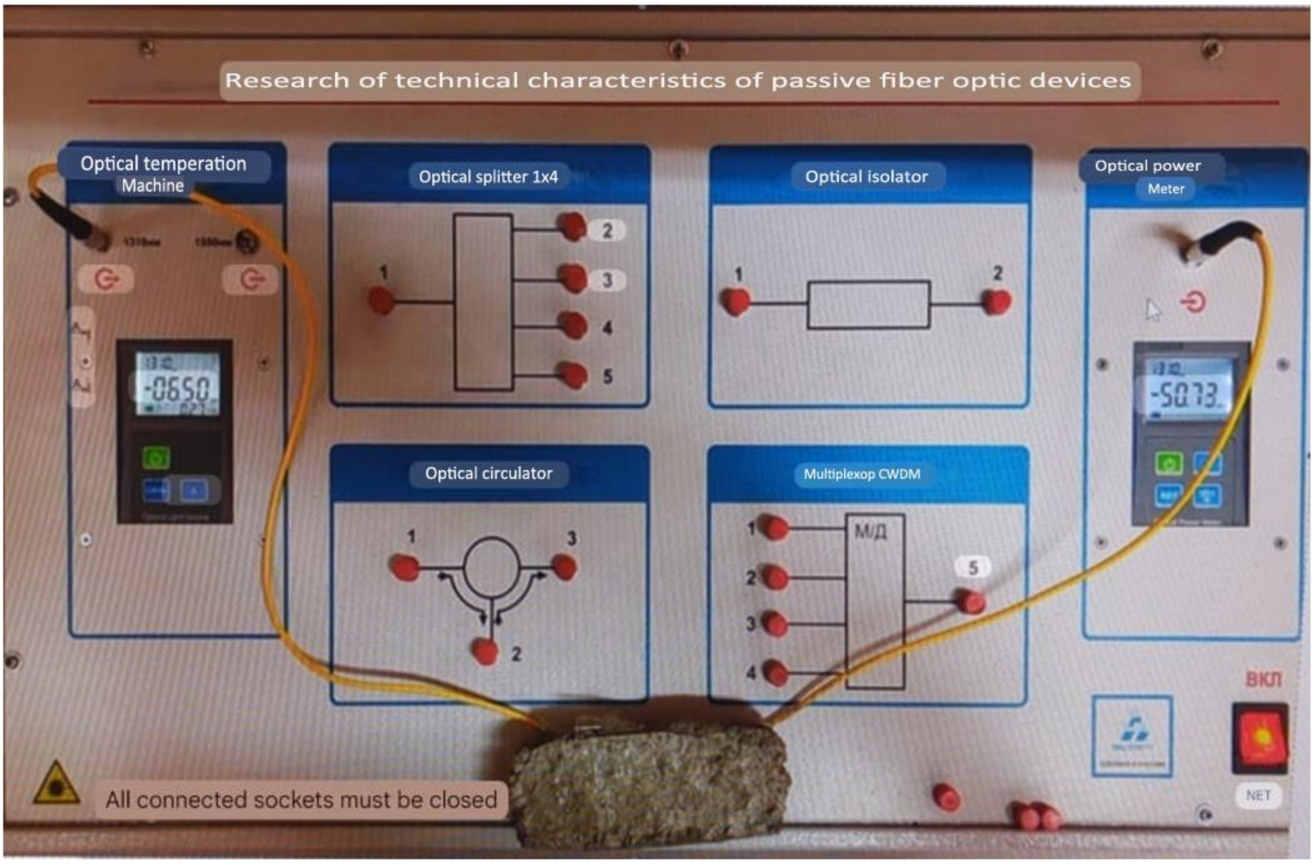

Figure 13.
Calculation of optical power when subjected to optical deformation.

Table 5 presents the wavelengths of 1310 nm the sampling frequency, the input signal level, and the output signal level at which it integrates with the concrete and deforms.

Table 5.
Results at 1310nm wavelength.

Input1310nm	Output 1310nm
0.27kHz – 6.50dBm	50.73dBm
100kHz – 6.50dBm	50.87 dBm
200kHz – 6.50dBm	51.04dBm

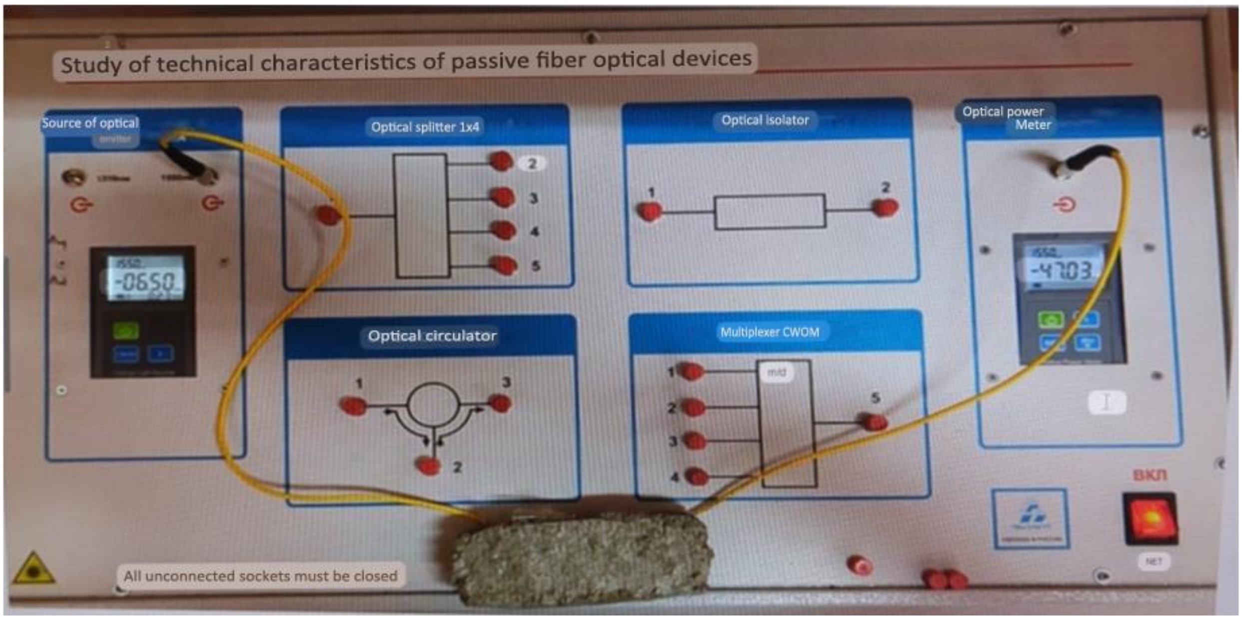

Figure 14.
Calculation of optical power when subjected to optical deformation.

Table 6 presents the wavelengths of 1550 nm the sampling frequency, the input signal level, and the output signal level at which it integrates with the concrete and deforms.

Table 6.
Results at 1550nm wavelength.

Input 1550nm	Output 1550nm
0.27kHz – 6.50dBm	47.03dBm
100kHz – 6.50dBm	47.13 dBm
200kHz – 6.50dBm	47.24dBm

Conclusion: By conducting research, we determined the optical power of the optical cable when subjected to some deformation. We notice that the power unit in optical data transmission systems increases as the vibration frequency increases during signal transmission (Figures 13-14).

The scientific stand "Study of the characteristics of optical fiber light guides" provides a unique opportunity to master the basics of the physical principles of the functioning of fiber-optic communication systems. The stand allows you to study in depth the modern element base used in fiber optics and laser measuring systems. The methodology for studying the structure of materials used in optical fibers is also presented in detail at this stand. The technical aspects of the formulation of research tasks are analyzed taking into account the physical principles of the methods, as well as the technical capabilities of the equipment used. Continuing these studies, the next study aims to delve into the fundamental physical principles of the fiber-optic communication systems, examine the internal structure of optical communication cables in fiber-optic and laser measurement systems, and to investigate deformed cables. Figures 15-17 show the process and steps of our experiment to investigate the parameters of optical fibers.

Figure 15.
Study of the internal structure of a deformed optical cable.

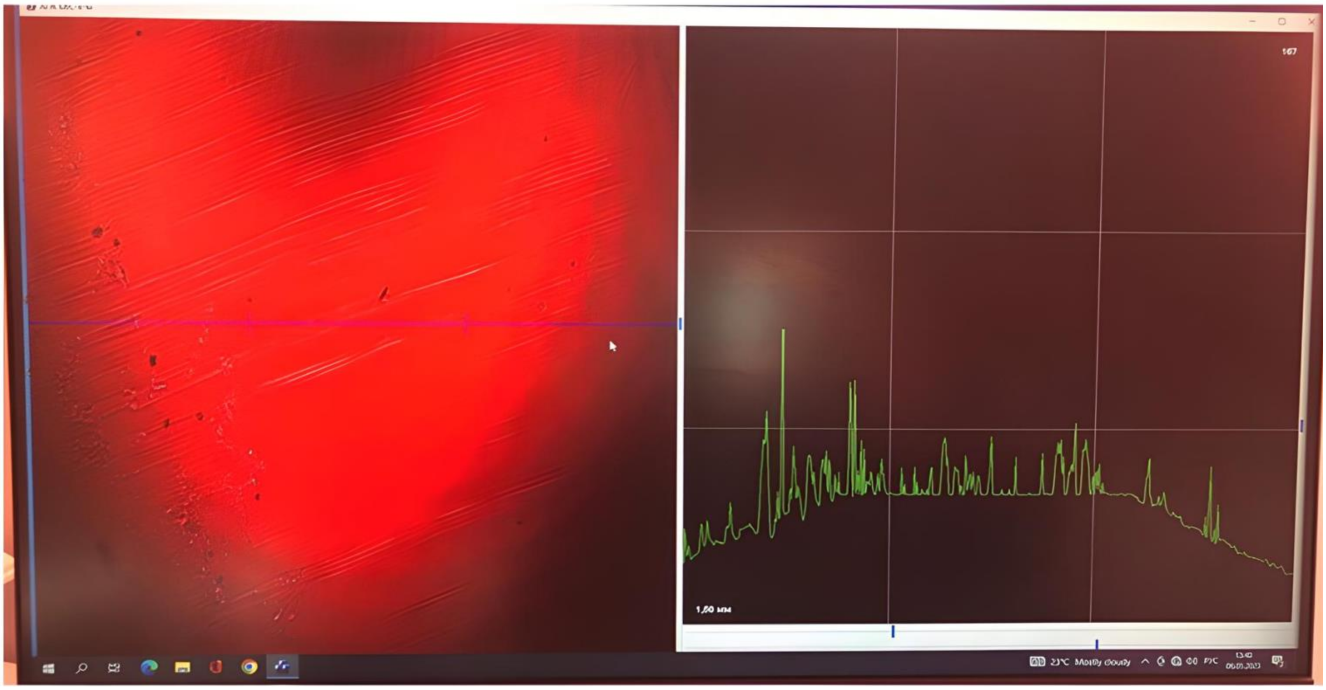

Figure 16.
Oscillogram of an optical fiber on a monitor.

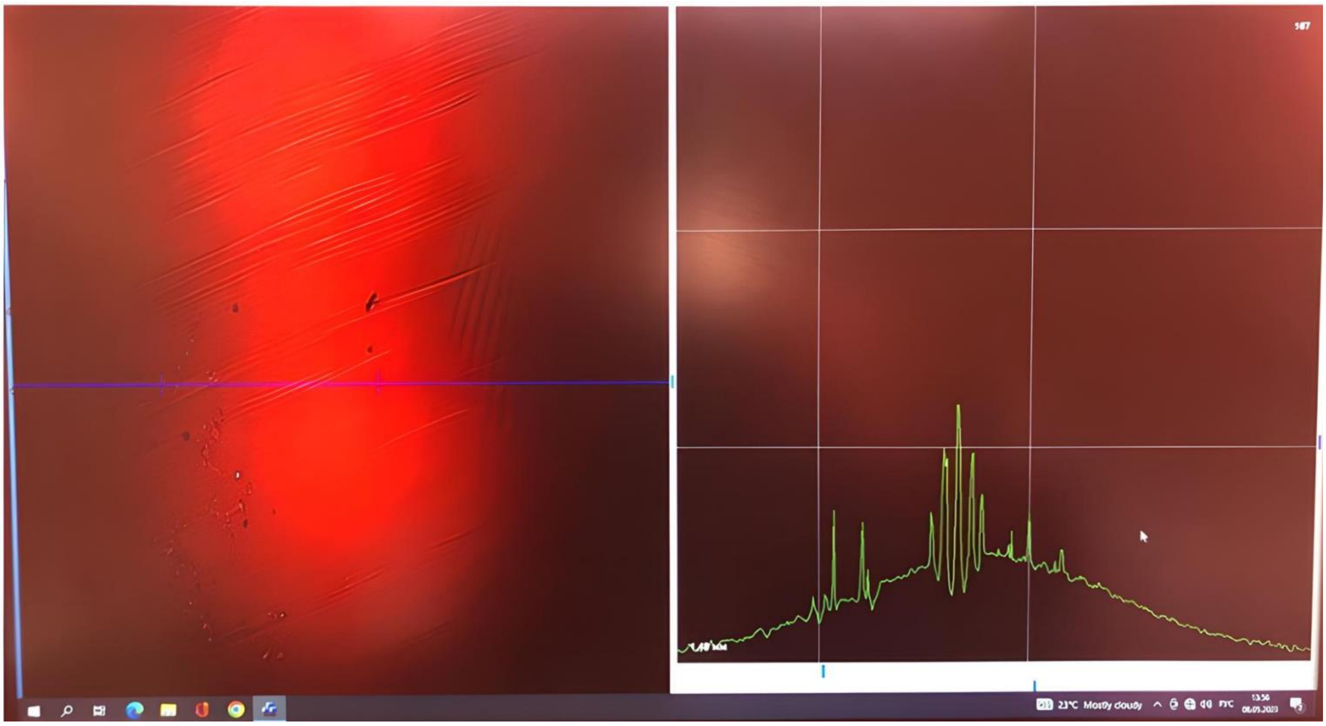

Figure 17.
Oscillogram of a deformed optical fiber on a monitor.

Concrete deformation of an optical fiber affects the signal transmission structure, as a comparison shows. It is possible to determine the angular importance of fiber insertion with the help of micrometric screws UV1 and UV2 to cover spots on the camera-related monitor screen and reduce its pulse on the oscillogram. In this case, we can correct the duplication of the focal zone of the lens, as well as the plane at the entrance of the fiber.

Since the parameters of the FBG change slowly, the main potential error may be insufficient measurement speed of the central wavelength to register high-speed pulse processes from a narrow-band radiation source, and in the case of a broadband radiation source, the power of the reflected signal from the VBR may be low, due to high-temperature instability.

Limitations in the study included a limited temperature range from 30 degrees Celsius to 130 degrees, which helped to maintain a high signal level and, accordingly, temperature stability, since this parameter is necessary for the ability of the FBG to maintain its original characteristics during and after exposure to high temperatures.

5. Conclusion

In this article, we considered the two-wave design that we demonstrated to determine temperature and strain for the study of a fiber-optic laser sensor. We calculated temperature and deformation using fiber-optic laser sensors. As a result of the analysis of the article, we analyzed many fiber-optic sensors. We carried out experimental work on temperature and deformation. Additional studies are analyzed to complete the tasks of the two experimental studies. The research results were obtained and shown in the OptiSystem program according to the optical signal versus temperature method scheme. According to the work result: when the temperature rises, the signal weakens and is deformed, which should not exceed the limit norms. The signal transmission structure of the optical sensor, subjected to deformation during the impact of concrete and such a fiber was considered and studied. In the optical power detection process, a higher vibration during signal transmission corresponds to a higher power unit in the optical data acquisition systems. In the future, the data obtained as a result of experiments can be used to determine the velocity shifts on metal and concrete surfaces.

Research on dual-wavelength fiber laser sensors for temperature and strain monitoring of concrete structures represents a significant advance in the field of infrastructure monitoring. The main scientific innovation lies in the combination of dual-wave technology with fiber optics, which provides simultaneous temperature and strain measurements with high precision and spatial resolution. The development of dual-wave laser systems minimizes thermo-optical distortion, providing accurate and stable measurements at variable temperatures. The use of fiber-optic sensors allows for distributed monitoring along the entire length of a specific structure, which is the key to early detection of potential problems and increasing the reliability of infrastructure. Almaty, located in the south of Kazakhstan, belongs to the earthquake hazard zone. Over the past 100 years, the city has experienced several devastating earthquakes, including a magnitude 7.3 earthquake that killed more than 100 people. Concrete structures are exposed to various factors, including seismic loads. During an earthquake, concrete structures may deform or collapse, causing loss of life and property. The research work has practical implications for the effectiveness of dual-wavelength fiber laser sensors using the Bragg grating principle to monitor the condition of concrete structures in real-time. This allows us to assess the degree of damage to buildings and structures and make plans for their restoration.

To clarify the experimental results and check their accuracy, laboratory tests with dual-wave fiber laser sensors were conducted on concrete samples. We simulated thermal and mechanical processes in a real structure using numerical methods, including finite element analysis, to optimize the structure and understand the influence of factors on sensor measurements. To confirm the accuracy and effectiveness of the proposed method while studying the internal structure of the structure, with data obtained by temperature and strain measurement methods, a dual-wave fiber laser comparative analysis of measurement results of sensors was carried out.

The data obtained as a result of this paper can be used to design monitoring systems for cooling towers for thermal power plants (TPP) and nuclear power plants (NPP). This would simplify the maintenance of the cooling towers and the timely detection of defects in them. Scientists and students will use the resulting layout to conduct further research in the field of metal coatings and concrete structures. The result of the study is potentially applicable to scientific areas in the fields of space technologies and oil well processing. It is planned to build a 3-D model of the NPP Cooling Tower with a built-in Bragg grid and simulate the operation of the NPP. And using the data obtained from this work, we can determine the temperature variation and deformation of the cooling tower.

References

[1] K. Guo, J. He, G. Xu, and Y. Wang, "Dual-polarization distributed feedback fiber laser sensor based on femtosecond laser-inscribed in-fiber stressors for simultaneous strain and temperature measurements," *IEEE Access*, vol. 8, pp. 97823-97829, 2020. https://doi.org/10.1109/ACCESS.2020.2997918

[2] K. Krzempek *et al.*, "ll-Fiber source for generation of tunable broadband fCEO-free Mid-IR pulses for laser spectroscopy applications," presented at the 2019 Conference on Lasers and Electro-Optics Europe & European Quantum Electronics Conference (CLEO/Europe-EQEC), IEEE, 2019.

[3] K. Krzempek, G. Dudzik, and K. Abramski, "Photothermal gas sensor in an intracavity mode-locked fiber laser configuration," presented at the 2019 Conference on Lasers and Electro-Optics Europe & European Quantum Electronics Conference (CLEO/Europe-EQEC), Munich, Germany, 2019.

[4] K. Guo *et al.*, "High-spatial-resolution high-temperature sensor based on ultra-short fiber Bragg gratings with dual-wavelength differential detection," *Journal of Lightwave Technology*, vol. 40, no. 7, pp. 2166-2172, 2021. https://doi.org/10.1109/jlt.2021.3131499

[5] A. Theodosiou, P. Savva, E. Mendoza, M. F. Petrou, and K. Kalli, "In-situ relative humidity sensing for ultra-high-performance concrete using polymer fiber bragg gratings," *In IEEE Sensors Journal*, vol. 21, no. 14, pp. 16086-16092, 2021. https://doi.org/10.1109/JSEN.2021.3075609

[6] D. H. Alustiza, N. A. Russo, M. Mineo, A. López, and Y. A. V. Zaccardi, "Packaging design assessment for an experimental fiber optic humidity sensor embeddable in concrete structures," presented at the In 2022 IEEE Biennial Congress of Argentina (ARGENCON), 2022.

[7] M. R. Islam, M. Bagherifaez, M. M. Ali, H. K. Chai, K.-S. Lim, and H. Ahmad, "Tilted fiber bragg grating sensors for reinforcement corrosion measurement in marine concrete structure," *In IEEE Transactions on Instrumentation and Measurement*, vol. 64, no. 12, pp. 3510-3516, 2015. https://doi.org/10.1109/TIM.2015.2459511

[8] M. H. B. Afzal, S. Kabir, and O. Sidek, "Fiber optic sensor-based concrete structural health monitoring," presented at the In 2011 Saudi International Electronics, Communications and Photonics Conference, 2011.

[9] I. O. Khramov, R. I. Shaidullin, and O. A. Ryabushkin, "Curved copper-coated optical fiber sensor for precise laser power measurements," presented at the International Conference Laser Optics (ICLO), St. Petersburg, Russia, 2020.

[10] S. I. Krivosheev, S. G. Magazinov, D. V. Kiesewetter, S. Z. Koshkinbayev, N. K. Smailov, and E. Ostropiko, "Adaptation of optical methods for recording high-speed displacements initiated by pulsed magnetic field," presented at the Conference of Russian Young Researchers in Electrical and Electronic Engineering (ElConRus), Saint Petersburg, Russian Federation, 2022.

[11] X. Xu, "Ultra-high-temperature sensors based on sapphire fiber bragg gratings created with femtosecond laser direct writing technique," presented at the 20th International Conference on Optical Communications and Networks (ICOCN), Shenzhen, China, 2022.

[12] A. Theodosiou, "Er/Yb double-clad fiber laser with fs-laser inscribed plane-by-plane chirped FBG laser mirrors," *In IEEE Photonics Technology Letters*, vol. 31, no. 5, pp. 409-412, 2019. https://doi.org/10.1109/LPT.2019.2896896

[13] P. Mikhailov, Z. Ualiyev, A. Kabdoldina, N. Smailov, A. Khikmetov, and F. Malikova, "Multifunctional fiber-optic sensors for space infrastructure," *Eastern-European Journal of Enterprise Technologies*, vol. 5, no. 113, pp. 80–89, 2021. https://doi.org/10.15587/1729-4061.2021.242995

[14] Steam-Assisted, "Steam-assisted gravity drainage," Retrieved: https://en.wikipedia.org/wiki/Steam-assisted_gravity_drainage. [Accessed 2020.

[15] Fiber-Optic Distributed, "Fiber-optic distributed temperature sensors help extend well life and increase re-covery," Retrieved: https://www.slb.com/resource-library/case-study/co/wellwatcher-briteblue-canada. [Accessed 2020.

[16] C.-Y. Hong, Y.-F. Zhang, G.-W. Li, M.-X. Zhang, and Z.-X. Liu, "Recent progress of using Brillouin distributed fiber optic sensors for geotechnical health monitoring," *Sensors and Actuators A: Physical*, vol. 258, pp. 131-145, 2017. https://doi.org/10.1016/j.sna.2017.03.017

[17] A. Torres, S. Diaz, O. Fuentes, J. Corres, I. Del Villar, and I. R. Matías, "Live Demonstration: Highly sensitive hollow-core fiber optic sensor using a ring laser for measuring material thermal expansion," *IEEE Sensors, Sydney, Australia*, pp. 1-1, 2021. https://doi.org/10.1109/SENSORS47087.2021.9639853

[18] K. Yang, "All-fiber orbital angular momentum laser generated with titled fiber bragg grating pair written in few-mode ring-core fiber," presented at the Optical Fiber Communications Conference and Exhibition (OFC), San Diego, CA, USA, 2019.

[19] M. Ding, D. Fan, W. Wang, Y. Luo, and G. D. Peng, *Basics of optical fiber measurements. In Handbook of Optical Fibers*. Singapore: Springer, 2019, pp. 1099-1137.

[20] L. Talbot, T. Boilard, and M. Bernier, "Fiber laser pump reflector based on volume bragg grating," presented at the Conference on Lasers and Electro-Optics Europe & European Quantum Electronics Conference (CLEO/Europe-EQEC), Munich, Germany, 2019, 2019.

[21] X. Zhao, Y. Wang, C. Liao, G.-D. Peng, Y. Gong, and Y. Wang, "Polymer-coated hollow fiber optofluidic laser for refractive index sensing," *Journal of Lightwave Technology*, vol. 38, no. 6, pp. 1550-1556, 2019. https://doi.org/10.1109/jlt.2019.2953137

[22] W. Zhang, R. Ma, Y. Ma, C. Hao, and Y. Song, "Fiber optic magnetic field sensor utilizing DFB fiber laser and terfenol-d material," presented at the 2018 Asia Communications and Photonics Conference (ACP), Hangzhou, China, 2018.

[23] L. Huang *et al.*, "Sub-kHz-linewidth wavelength-tunable single-frequency ring-cavity fiber laser for C-and L-band operation," *Journal of Lightwave Technology,* vol. 39, no. 14, pp. 4794-4799, 2021. https://doi.org/10.1109/jlt.2021.3074824

[24] D. Kiesewetter *et al.*, "Application of fiber bragg gratings as a sensor of pulsed mechanical action," *Sensors,* vol. 22, no. 19, p. 7289, 2022. https://doi.org/10.3390/s22197289

[25] D. Kiesewetter, S. Krivosheev, S. Magazinov, V. Malyugin, S. Koshkinbayev, and N. Smailov, "Measurement of high-speed deformations using fiber bragg gratings," presented at the 2022 International Conference on Electrical Engineering and Photonics (EExPolytech), IEEE, 2022.

[26] J. He *et al.*, "Slit beam shaping for femtosecond laser point-by-point inscription of highly localized fiber Bragg grating," *Journal of Lightwave Technology,* vol. 40, no. 16, pp. 5722-5728, 2022. https://doi.org/10.1109/jlt.2022.3182319

[27] F. Zhang, S. Jiang, X. Zhang, C. Wang, J. Ni, and G. Peng, "Ultra-thin fiber laser hydrophone with static pressure equalization and improved response," *IEEE Photonics Technology Letters,* vol. 31, no. 24, pp. 1968-1970, 2019. https://doi.org/10.1109/lpt.2019.2951776

[28] Z. Lou *et al.*, "Realization of in situ fiber-core temperature measurement in a kilowatt-level fiber laser oscillator: Design and optimization of the method based on OFDR," *Journal of Lightwave Technology,* vol. 39, no. 8, pp. 2573-2582, 2021. https://doi.org/10.1109/jlt.2020.3048747

[29] A. Kabdoldina *et al.*, "Development of the design and technology for manufacturing a combined fiber-optic sensor used for extreme operating conditions," *Eastern-European Journal of Enterprise Technologies,* vol. 119, no. 5, pp. 34–43, 2022.

[30] M. Feng *et al.*, "Mode-locked Tm^{3+}-doped fiber laser with CV mode output using a cascading chirped LPFG," *IEEE Photonics Technology Letters,* vol. 32, no. 24, pp. 1523-1526, 2020. https://doi.org/10.1109/lpt.2020.3038415

[31] J. BE, "Optical fibre sensors using wavelength modulation and simplified spectral analysis," *Journal of Scientific Instruments,* vol. 17 p. 1240, 1984.

[32] B. Zhumazhanov *et al.*, "Modeling the method for determining the stimulated brillouin scattering threshold in a single-mode optical fiber," *Eastern-European Journal of Enterprise Technologies,* vol. 1, no. 5, p. 115, 2022. https://doi.org/10.15587/1729-4061.2022.253390

[33] Y. Liu *et al.*, "Liquid-core-microtubule-enhanced Laser sensor for high resolution temperature measurement," *IEEE Sensors Journal,* 2023. https://doi.org/10.1109/jsen.2023.3278092

[34] S. Orazaliyeva, G. Kadirbayeva, and K. Chezhimbayeva, "Evaluation of the effectiveness of the effect of photosensitization on the spectral characteristics of the fiber bragg grating," *Eastern-European Journal of Enterprise Technologies,* vol. 117, no. 5, pp. 1-6, 2022. https://doi.org/10.15587/1729-4061.2022.259033

[35] K. Liu *et al.*, "Broadband vibration sensor using reflected excessively tilted fiber grating with clamped beam," *IEEE Photonics Technology Letters,* vol. 33, no. 8, pp. 379-382, 2021. https://doi.org/10.1109/lpt.2021.3064574

[36] P. O. Chibuike, K. C. Odo, L. U. Omeje, and T. Sutikno, "Output performance evaluation of the automatic voltage regulator system on pre-filter control technique," *International Journal of Power Electronics and Drive Systems,* vol. 14, p. 789, 2023. https://doi.org/10.11591/ijpeds.v14.i2.pp789-798

[37] M. Y. Lada, M. A. M. Radzi, J. Jasni, H. Hizam, A. Jidin, and S. H. Mohamad, "Performance of three-phase three-wire cascaded H-bridge multilevel inverter-based shunt active power filter," *International Journal of Power Electronics and Drive Systems,* vol. 2088, no. 8694, p. 1431, 2020. https://doi.org/10.11591/ijpeds.v11.i3.pp1430-1440

[38] S. Liao and T. Wong, "Optimal design of feedback-interferometric fiber laser sensors," *IEEE Sensors Journal*, vol. 19, no. 24, pp. 12016-12023, 2019. https://doi.org/10.1109/jsen.2019.2936222

[39] F. Karim, A. F. Mitul, B. Zhou, and M. Han, "High-sensitivity demodulation of fiber-optic acoustic emission sensor using self-injection locked diode laser," *IEEE Photonics Journal*, vol. 14, no. 4, pp. 1-10, 2022. https://doi.org/10.1109/jphot.2022.3192806

[40] N. Smailov *et al.*, "Numerical simulation and measurement of deformation wave parameters by sensors of various types,," *Sensors,* vol. 23, no. 22, p. 9215, 2023. https://doi.org/10.3390/s23229215

[41] A. Kuttybayeva, A. Sabibolda, S. Kengesbayeva, M. Baigulbayeva, A. Amir, and B. Sekenov, "Investigation of a fiber optic laser sensor with grating resonator using mirrors," presented at the 2024 Conference of Young Researchers in Electrical and Electronic Engineering (ElCon), Saint Petersburg, Russian Federation, 2024.

[42] G. Kadirbayeva, K. Chezhimbayeva, M. Khizirova, and W. Wójcik, "Application of the method of measuring deformation parameters under mechanical action on concrete beams using a fiber bragg grating," *Eastern-European Journal of Enterprise Technologies,* vol. 124, no. 7, pp. 54-62, 2023.

[43] A. Kalizhanova, M. Kunelbayev, W. Wojcik, and A. Kozbakova, "Experimental study of a temperature measurement system for an overhead power line using sensors based on TFBG," *International Journal of Innovative Research and Scientific Studies,* vol. 7, no. 1, pp. 180-188, 2024. https://doi.org/10.53894/ijirss.v7i1.2596